Radiotherapy and Oncology xxx (2015) xxx–xxx

Contents lists available at ScienceDirect

Radiotherapy and Oncology

journal homepage: www.thegreenjournal.com

Original article

An image guided small animal radiation therapy platform (SmART) to monitor glioblastoma progression and therapy response

Sanaz Yahyanejad [a,1], Stefan J. van Hoof [a,1], Jan Theys [a,1], Lydie M.O. Barbeau [a], Patrick V. Granton [b], Kim Paesmans [a], Frank Verhaegen [a], Marc Vooijs [a,*]

[a] Department of Radiotherapy (MAASTRO)/GROW – School for Developmental Biology & Oncology, Maastricht University, The Netherlands; and [b] Department of Oncology, London Health Sciences Center, Canada

ARTICLE INFO

Article history:
Received 17 April 2015
Received in revised form 11 June 2015
Accepted 15 June 2015
Available online xxxx

Keywords:
Glioblastoma
Small animal radiation
3D model
Image guided
Temozolomide
Micro-CT

ABSTRACT

Background and purpose: Glioblastoma multiforme is the most common malignant brain tumor. Standard treatment including surgery, radiotherapy and chemotherapy with temozolomide is not curative. There is a great need for *in vitro* and *in vivo* models closely mimicking clinical practice to ensure better translation of novel preclinical findings.

Methods and materials: A 3D spheroid model was established using the U87MG cell line. The efficacy of temozolomide, RT and combinations was assessed using growth delay assays. Orthotopic glioblastoma tumors were established, different radiation doses delivered based on micro-CT based treatment planning (SmART-plan) and dose volume histograms (DVH) were determined. Tumor growth was monitored using bioluminescent imaging.

Results: 3D spheroid cultures showed a dose-dependent growth delay upon single and combination treatments. Precise uniform radiation was achieved in all *in vivo* treatment groups at all doses tested, and DVHs showed accurate dose coverage in the planning target volume which resulted in tumor growth delay.

Conclusion: We demonstrate that 3D spheroid technology can be reliably used for treatment efficacy evaluation and that mimicking a clinical setting is also possible in small animals. Both these *in vitro* and *in vivo* techniques can be combined for clinically relevant testing of novel drugs combined with radiation.

Glioblastoma multiforme (GBM) is the most common malignant brain tumor in adults. The current standard of care includes surgery followed by radiotherapy (RT) and chemotherapy using temozolomide (TMZ) with median survival after diagnosis of 15 months [1]. TMZ acts via alkylation of O^6-Guanine, which induces DNA damage and cell death. However, many patients are observed to acquire TMZ resistance in recurrent gliomas [2]. Therefore, there is an urgent need for reliable *in vitro* and preclinical models that more closely model the course of human GBM and enable testing of new interventions that improve clinical management and are predictive for disease outcome in patients.

Increasing evidence shows that some drugs that fail to show efficacy in 2D are effective in 3D culture systems [3]. This is significant because spheroids better recapitulate features of solid tumor growth such as inward proliferation and spatiotemporal changes in oxygen concentration reminiscent of tumor hypoxia [4]. Radiation sensitivity is also known to be different between cells grown as monolayer or cells grown in 3D [5]. Therefore, spheroids may be a more relevant *in vitro* model system to perform drug screening in combination with radiotherapy.

Through these 3D spheroid model systems, once candidate drugs have been identified, preclinical animal models can improve their translational relevance e.g. by reflecting the tumor micro-environment, especially when the clinical treatment practice can be mimicked by use of orthotopic tumor models and precision image-guided radiotherapy, downscaled from human radiotherapy conditions. Orthotopic mouse models require non-invasive imaging techniques to monitor disease progression and therapy response longitudinally. Bioluminescence imaging (BLI) is a fast and sensitive method to monitor tumor growth kinetics *in vivo*. Recently, dedicated image-guided small animal radiotherapy (SmART) devices have become available for preclinical research, which combine micro-CT imaging or other modalities

* Corresponding author at: Dept. of Radiotherapy (MaastRO)/GROW – School for Developmental Biology and Oncology, Maastricht University, Universiteitssingel 50, 6229 ER Maastricht, The Netherlands.

E-mail address: marc.vooijs@maastrichtuniversity.nl (M. Vooijs).

[1] These authors contributed equally to this work.

http://dx.doi.org/10.1016/j.radonc.2015.06.020
0167-8140/

(e.g. BLI) with advanced precision irradiation using millimeter sized beams in the same frame of reference making tumor delineation and treatment planning highly accurate thereby limiting normal tissue toxicity [6]. Previously, we have shown that combining BLI with contrast-enhanced micro-CT provides an accurate and sensitive integrated approach to determine in situ tumor volumes and monitoring of disease progression in an orthotopic model of GBM [7]. The focus of this study was to develop a clinically relevant integrated approach using a spheroid drug screening platform *in vitro* and to demonstrate the power of using high-precision SmART technology *in vivo* to assess the effect of radiation treatment in a model of intracranial GBM.

Materials and methods

Cells and chemical treatments

U87MG-Luc2 and U87MG-R (resistant cells to TMZ) cells were grown in DMEM (Invitrogen) supplemented with 10% FBS (Hyclone). U87MG-Luc2 is a widely used glioma cell line transduced with a lentiviral vector expressing firefly luciferase (Perkin Elmer, Waltham, MA). Temozolomide resistant U87MG-R were generated essentially as described [8]. Cell lines were treated with increasing concentration of TMZ (Selleck) (1, 5 and 25 μM) and/or Cisplatin (Selleck) (2.5 μM). DMSO was used as vehicle for both drugs. TMZ and Cisplatin were stored at 100 mM stock concentration in −80 and room temperature, respectively.

3D spheroid assay

0.750 gr agarose (Sigma–Aldrich) was dissolved in 50 ml serum free medium and autoclaved. 50 μl of agarose mixture was pipetted per well into the 96-well plate. 2500 cells/200 μl of growth medium were seeded on the agarose coated plates per well. After 4 days, one spheroid per well was formed with a diameter of ~400 μm (12 spheroids/treatment condition), treatment was started and phase-contrast pictures were taken from individual spheroids 3×/week. Spheroid volumes were analyzed using Matlab (Mathworks). Growth medium with drugs was refreshed every 3 days.

Animal surgery and imaging

Immunocompromised CD1 nu/nu mice ($n = 23$) were used in this study. Animal work was performed in accordance with national code for the experimentation with animals. Surgical procedures and imaging techniques were performed as described previously [7]. All mice were anesthetized with a gas mixture of air and 4% isoflurane prior to intracranial surgery. A midline scalp incision was made, the bregma was identified and the guide screw entry was then marked at 3 mm posterior and 2 mm right lateral to the bregma and from the cortical surface a 3 mm deep craniotomy was created. 5 μl cell suspension in PBS (100,000 cells) was injected into the brain using a Hamilton syringe. The needle was slowly removed 5 min after the injection to prevent any reflux of the cells. The skin was closed using skin glue. BLI and contrast-enhanced micro-CT imaging were used to confirm tumor establishment. BLI was performed 3×/week using the Optix MX2 system (ART Inc., Saint-Laurent, QC). Fifteen minutes prior to BLI imaging, 150 mg/kg of d-luciferin (PerkinElmer, Waltham, MA) in PBS was injected intraperitoneally. Images were analyzed using Optix (OptiView version 2.01, ART Inc.). Micro-CT imaging was performed periodically using the small animal micro-IR (X-RAD 225Cx, Precision X-ray Inc., North Branford, CT). To enhance soft tissue contrast 150 μL of the iodinated Omnipaque 350 (GE Healthcare, Little Chalfont, UK) was injected undiluted via the tail vein immediately prior to micro-CT imaging.

In vivo irradiation

The dedicated small animal radiotherapy planning system SmART-Plan (version 1.3.1, Precision X-ray, North Branford, CT) was used to create, evaluate, and deliver irradiation [9]. The tumor was delineated as gross target volume (GTV) and the normal brain was delineated as organ at risk (OAR). The Planning Target Volume (PTV) was equal to the GTV and dose was planned to the PTV. Two static parallel opposed beams linked to the irradiator isocenter, were used to deliver a homogeneous dose to the PTV. Radiation was delivered using a photon spectrum of 225 kVp at 12 mA, which provides a dose rate of approximately 3 Gy/minute.

Statistical analysis

Statistical analysis was carried out using GraphPad Prism version 5.01. A non-parametric Mann Whitney and one way ANOVA was performed to determine differences in growth delay *in vitro* and *in vivo*, respectively. Asterisk indicates significance ($^{*}p < 0.05$, $^{**}p < 0.01$ and $^{***}p < 0.001$), ns: not significant.

Results

We established robust spheroid culturing conditions for U87MG-Luc2 cells that yield highly reproducible sphere growth reliable for quantitative treatment efficacy evaluation. Spheres could be maintained in culture for as long as 25 days and reaching up to at least 20 times of their initial treatment starting volume.

We first determined the sensitivity of U87MG-Luc2 spheroids to different concentrations of TMZ. Use of increasing concentrations of TMZ (1, 5 and 25 μM) resulted in a significant increase in spheroid growth delay expressed as time to reach 15 times starting volume (T15SV) from 8 days for vehicle to 8.1, 8.8 and 9.8 days, respectively (Fig. 1A). Such TMZ dose-dependent response was not observed in U87MG-R cells (Fig. 1B). We chose 5 μM TMZ as a sub-curative dose for use in combination treatments. In U87MG-Luc2 cells single radiation doses of 2, 4, 8 and 12 Gy resulted in a dose-dependent decrease in T15SV from 4.3 days in the non-irradiated group to 5.0 and 5.9 days after 2 and 4 Gy, respectively. Doses of 8 and 12 Gy resulted in such a severe growth delay that 15SV could not be reached within the course of the experiment. Although the growth rate of the U87MG-R was slower, the response to RT was similar, in that there was an increasing growth delay after 2, 4, 8 and 12 Gy irradiation (Fig. 1D). We then tested the combination treatments and found that addition of TMZ (5 μM) resulted in additive effects at every radiation dose level in the U87MG-Luc2 cells (Fig. 1C), but not in the U87MG-R cells. If anything, addition of TMZ seemed to make the cells even slightly more radiation resistant (Fig. 1D). These data show the potential of using 3D spheroid technology to reliably quantify treatment efficacy. Exemplified here using the standard treatment of care for GBM (radiation + TMZ), this methodology can now be applied to test virtually any treatment combination. One of such uncommon, but potentially interesting combination is addition of alkylating agents such as Cisplatin to the standard of care schedule. The addition of Cisplatin to the standard treatment combination in U87MG-Luc2 cells resulted in a significant ($p < 0.05$) increase in spheroid growth delay (Fig. 1E).

To forward novel treatment combinations into patients it is of vital importance not only to have a robust *in vitro* system for efficacy testing, but also to develop clinically relevant *in vivo* models and technology. To do so, we applied stereotactic implantation to intracranially inject U87MG-Luc2 cells. BLI measurements

Please cite this article in press as: Yahyanejad S et al. An image guided small animal radiation therapy platform (SmART) to monitor glioblastoma progression and therapy response. Radiother Oncol (2015), http://dx.doi.org/10.1016/j.radonc.2015.06.020

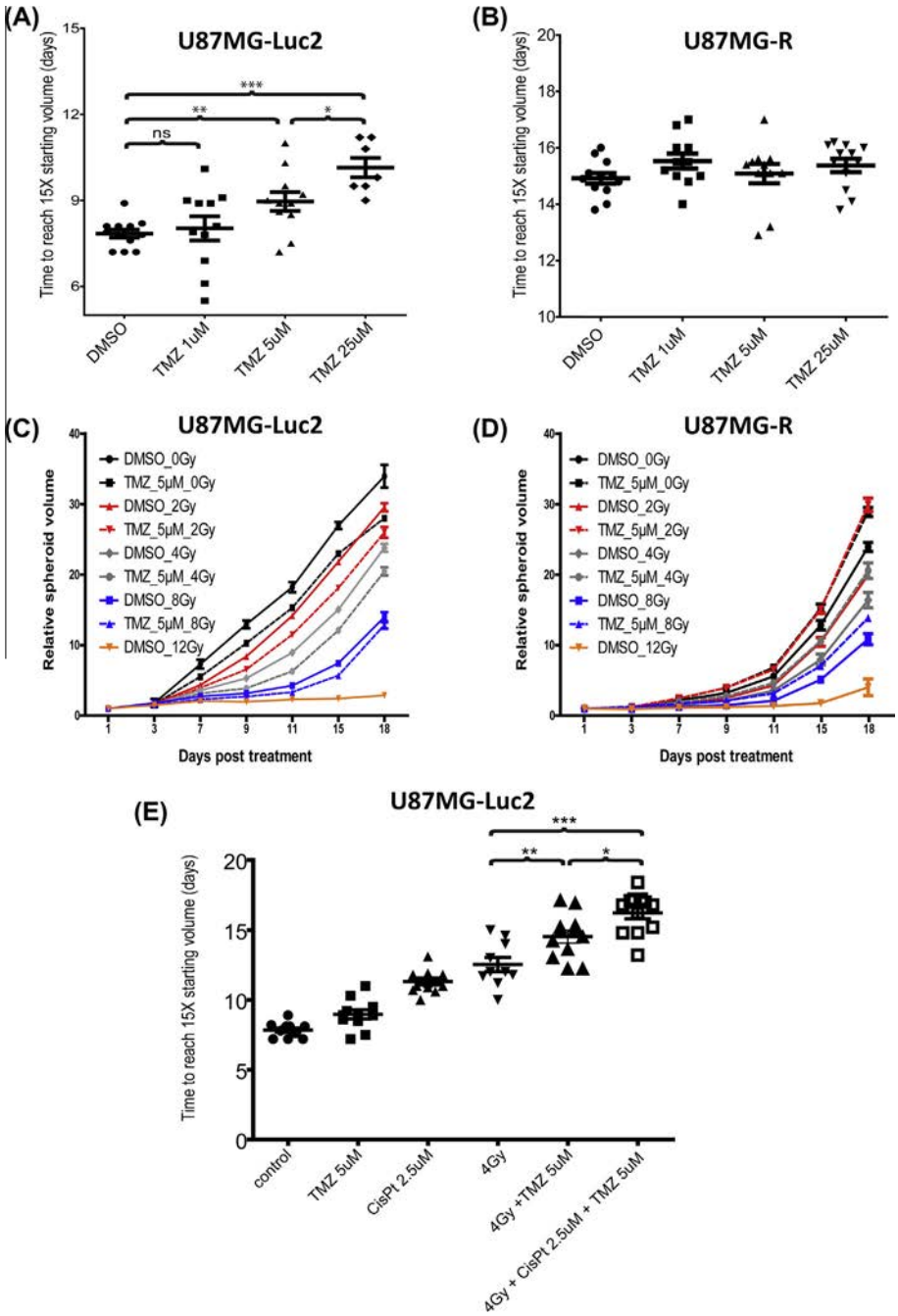

Fig. 1. Dose–response spheroid growth delay upon treatment with TMZ, RT and their combinations. (A and B) Increasing concentration of TMZ shows an enhanced growth delay for U87MG-Luc2, while no effect is observed in U87MG-R. (C) RT and RT + TMZ treatment shows an increased growth delay for U87MG-Luc2. (D) RT treatment shows an increased growth delay while RT + TMZ shows to reduce the delay. (E) RT + CisPt + TMZ shows an enhanced growth delay compared with RT and RT + TMZ. Spheroid growth delay is expressed in T15SV.

(3×/week) were used to monitor tumor growth. Having established the *in vivo* growth characteristics, we used SmART technology for precise irradiation. Prior to irradiation, tumors were delineated using contrast-enhanced micro-CT for planning the radiation delivery (Fig. 2B). Upon 3 consecutive increases of BLI signal, indicative of active tumor growth, tumors were irradiated with either of 4, 8 or 12 Gy, based on treatment plans generated using SmART-plan. An example of tumor delineation in axial, coronal and sagittal direction is shown with radiation treatment set-up using 2 parallel-opposed beams (Fig. 2A). Tumors were irradiated with 5 mm or 3 mm beams, depending on their volume. Resulting dose-volume histograms (DVH) and DVH metrics of the PTV and OAR for all *in vivo* irradiations are shown in Table 1. The DVHs indicate clearly that the prescribed dose to the PTV is well achieved, and reveal that about 80% of the normal brain remains untreated (Fig. 3). The mean dose within the PTV (D_{mean}) was close to the planned dose with an average prescribed dose of 4.0, 7.6 and 11.9 Gy for 4, 8 and 12 Gy radiation groups, respectively (Table 1). In one case, a high deviation from the planned dose of 8 Gy was observed. This was because the tumor volume was not completely covered by the 3 mm beam (Supplementary Fig. 1).

To assess the target coverage and normal tissue sparing, we report the V_{95} for the PTV and V_{100} for the OAR, i.e. the percentages of the volume receiving 95 (V_{95}) or 100 (V_{100}) % of the prescribed

Please cite this article in press as: Yahyanejad S et al. An image guided small animal radiation therapy platform (SmART) to monitor glioblastoma progression and therapy response. Radiother Oncol (2015), http://dx.doi.org/10.1016/j.radonc.2015.06.020

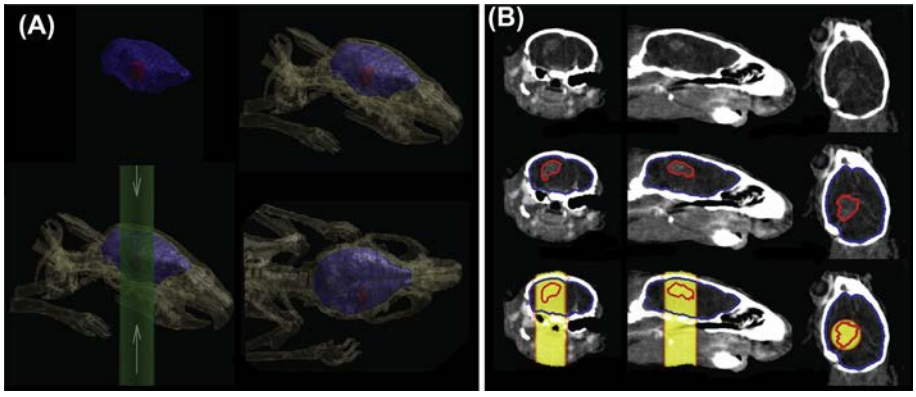

Fig. 2. Radiation treatment set-up. (A) Visualization of the tumor in the brain from different plane and applied parallel opposed beams to target the tumor. (B) Tumor delineation based on contrast-enhanced micro-CT prior to RT. Red line: tumor, Blue line: normal brain.

Table 1
Dose–volume metrics and structure volumes for the PTV and healthy brain, and applied circular beam size of all cases, sorted per dose group. Average values are provided for each dose group.

Beam (mm)	PTV					Normal brain			
	D_{mean} (Gy)	D_5 (Gy)	D_{95} (Gy)	V_{95} (mm^3)	V (mm^3)	D_{mean} (Gy)	D_{max} (Gy)	V_{100} (%)	V (mm^3)
4 Gy									
5	4.1	4.3	3.9	98.2	4.0	0.9	4.6	9.0	324.1
5	4.0	4.2	3.9	99.5	11.0	0.9	4.4	7.7	345.9
3	4.2	4.4	3.9	99.8	4.1	0.5	4.7	6.3	338.4
5	4.0	4.1	3.8	92.5	6.7	0.7	4.4	1.7	348.5
5	–	–	–	–	–	0.8	4.6	6.8	341.2
5	3.9	4.1	3.8	91.4	9.3	0.9	4.3	1.9	364.3
Average	4.0	4.2	3.9	96.3	7.0	0.8	4.5	5.6	343.7
8 Gy									
3	7.9	8.3	7.6	93.4	2.6	1.1	9.0	2.6	338.4
3	6.6	8.1	1.2	42.6	12.7	1.0	8.8	1.5	406.1
5	7.9	8.3	7.5	89.3	6.5	1.7	8.9	4.0	336.0
5	–	–	–	–	–	1.9	9.5	11.3	331.4
5	8.1	8.5	7.7	98.4	2.7	2.0	9.2	10.5	380.9
Average	7.6	8.3	6.0	80.9	6.1	1.6	9.1	6.0	358.5
12 Gy									
5	12.2	12.9	11.6	98.6	6.7	2.8	14.1	11.1	336.9
3	11.6	12.1	11.0	69.3	2.6	1.4	12.8	0.3	333.0
5	12.2	12.9	11.6	98.5	9.7	2.7	13.8	8.9	344.2
5	12.1	12.6	11.6	97.0	13.0	2.9	13.5	10.2	354.4
3	11.6	12.6	10.6	60.4	5.6	2.4	14.5	2.9	376.8
5	–	–	–	–	–	2.5	13.6	5.1	341.5
3	11.6	12.1	11.0	70.5	1.3	1.6	12.7	0.4	335.9
Average	11.9	12.5	11.2	82.4	6.5	2.3	13.6	5.6	346.1

dose. To provide additional insight in the uniformity of the delivered dose to the PTV, we report the minimum dose to the hottest 5% (D_5) and 95% (D_{95}) of the PTV. The uniformity is consistent among mice in each radiation group, with only one case showing a large variation due to the aforementioned reason. We observed that on average, 96.3%, 80.9%, and 82.4% of the tumor volume prescribed with the planned doses of 4, 8 and 12 Gy, respectively, received 95% of the prescribed doses (V_{95}). We noticed that mice irradiated with 3 mm beams showed lower V_{95} compared to 5 mm ones (Table 1). Three mice are lacking information on their PTV due to erroneous injection of the contrast agent for the CT image; however the BLI demarcated signal region was used for irradiation using the 5 mm beam, which could provide a sufficient margin to achieve good tumor coverage.

To standardize tumor burden the endpoint was defined as the time to reach 10 times increase in absolute number of photons measured by BLI. Radiation treatment showed a significant dose–response on tumor growth delay measured from an average of 16 days for non-irradiated group to 22.7, 26.3 and 28.1 days for mice receiving a single dose of 4,8 and 12 Gy, respectively (Fig. 4A). By increasing the dose, differences were observed in the survival based on humane endpoints as expressed in the survival curves (Fig. 4B).

Discussion

The micro-invasive nature of GBM into the normal brain makes complete surgical resection impossible, and standard of care for GBM includes radiotherapy and chemotherapy [1]. Advances in molecular imaging using CT-based planning PET [10] and MRI [11] have resulted in improved accuracy of treatment planning and a modest increase in tumor control with reduced normal tissue toxicities. However, more radical improvements on survival are needed and will most likely come from novel therapeutic approaches. To facilitate the rapid translation of radiobiology into clinical practice, novel approaches need to be validated in relevant *in vitro* as well as preclinical *in vivo* models using routine clinical procedures. Here we demonstrate an integrated platform for

Please cite this article in press as: Yahyanejad S et al. An image guided small animal radiation therapy platform (SmART) to monitor glioblastoma progression and therapy response. Radiother Oncol (2015), http://dx.doi.org/10.1016/j.radonc.2015.06.020

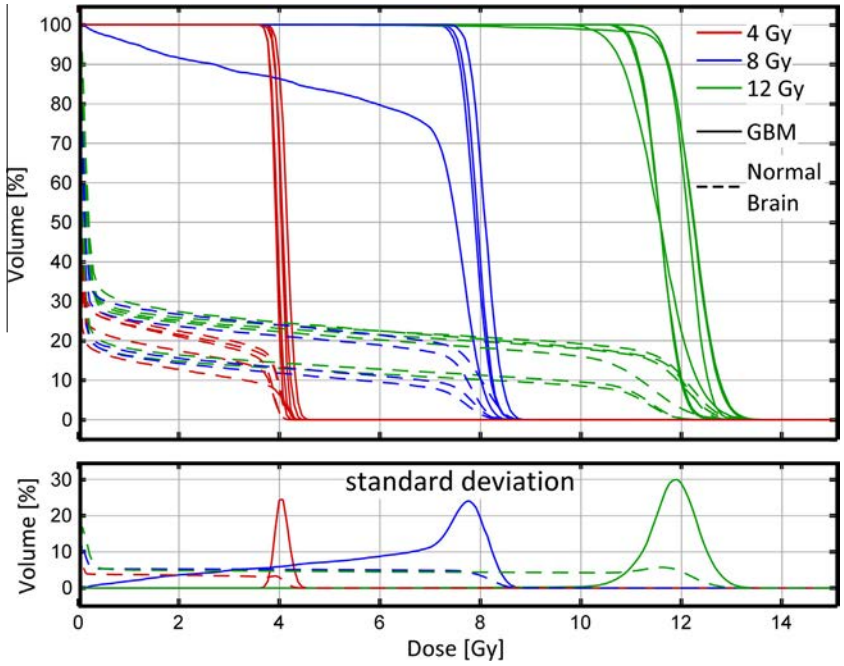

Fig. 3. Dose–volume histograms. (Top) Resulting DVHs of the tumors and normal brain tissue (excluding tumor) for all cases. (Bottom) Standard deviations of the DVHs per dose group.

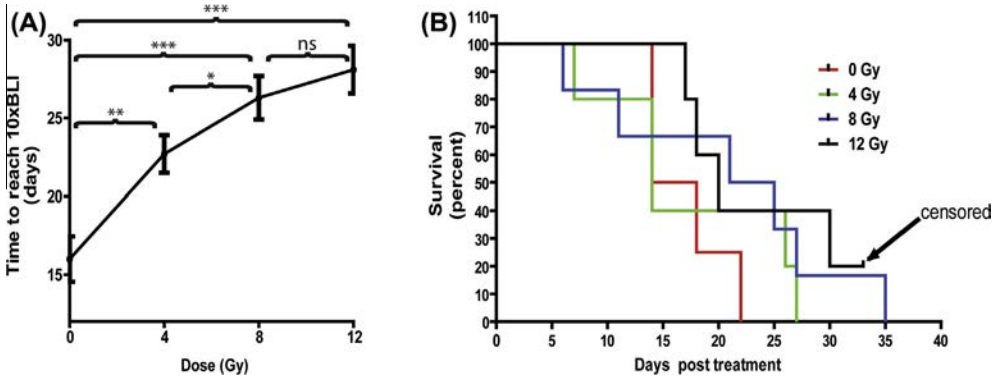

Fig. 4. Radiation dose–response tumor growth delay and Survival. (A) Tumor growth delay is normalized to the BLI signal intensity at the start of the treatment. (B) Kaplan–Meier curves showing times to reach endpoint measured by neurological and atypical behavior.

GBM treatment evaluation from *in vitro* drug screening of treatment combinations to *in vivo* orthotopic tumor model using small animal image guided radiotherapy planning and precision irradiation.

First our study confirms that the 3D spheroid model is a reproducible and robust screening methodology to identify combination therapies for GBM that reflect *in vivo* response. Dose–responses can be obtained in the spheroid growth delay assays using clinically relevant treatments and characteristics such as TMZ sensitivity and resistance. Gene expression profiles derived from 3D models are reported to be closer to clinical profiles when compared to 2D models [12]. Strong similarities have been shown in drug resistance phenotypes between tumor samples and those observed with 3D spheroid models [13].

These findings provide the rationale for using 3D system to better predict clinical efficacy. In that context, our data showing significant increased efficacy when combining TMZ/RT with Cisplatin are encouraging. Although not commonly used, the non-overlapping toxicity profiles of both drugs and the underlying mechanism of action whereby cisplatin reduces DNA-alkyl transferase enzyme activity (responsible for conferring resistance to TMZ) offer potential. The combination of Cisplatin with bid TMZ regimen in chemotherapy-naïve patients with recurrent glioblastoma has shown already to be effective in a Phase II clinical study [14]. Our data in spheroids indicate that adding Cisplatin has also potential in regimens where radiation is part of standard of care.

The 3D models used here however still lack important factors from the tumor micro-environment such as vasculature, fibroblasts or immune cells. Therefore, we used a preclinical orthotopic GBM model and demonstrated the feasibility of image-guided radiotherapy using clinical radiation schemes employing image-guided small animal micro-irradiators. While the U87MG model lacks important features of human GBM such as micro-invasion its reproducible tumor growth with short latencies make it an ideal preclinical model to study the *in vivo* efficacy of novel radiosensitizers in standard of care combination therapies. Models which have more typical GBM characteristics such as primary patient derived models represent important advances which need to be implemented. The effect of radiation on normal brain tissue is a determining factor in GBM treatment because of functional impairment. Considering this and in contrast to standard devices using a single large beam, the use of image-guided

Please cite this article in press as: Yahyanejad S et al. An image guided small animal radiation therapy platform (SmART) to monitor glioblastoma progression and therapy response. Radiother Oncol (2015), http://dx.doi.org/10.1016/j.radonc.2015.06.020

multiple cross-firing beams on a rotating gantry that delivers a prescribed dose to an isocenter placed at the center of the target (tumor) results in greater dose homogeneity and less dose at the OAR. Based on the DVHs, the parallel-opposed fields indicate that the beams were highly conformal to a localized brain region. They also demonstrate a highly uniform dose distribution across the tumor, which is particularly useful when trying to establish a dose–response curve in order to identify an appropriate treatment dose that allows room for therapeutic synergies for multimodal treatments. However, the fraction of the beam containing penumbra is greater for the smaller 3 mm beam than for the 5 mm beam, which reduced the V_{95}. Therefore, treatment margins should be applied to visible tumors (GTV) for sub-clinical disease spread and uncertainties in treatment delivery. Our study employed a radiation field size that is proportionally more realistic to clinical experience than previously published used whole brain irradiation, which is frequently used in mice.

In conclusion, the use of new high-precision image guided animal irradiation platforms may accelerate the discovery and facilitate the implementation of novel treatment interventions from *in vitro* screening approaches into clinical testing.

Conflict of interest

None.

Acknowledgements

M.V. and L.B. are supported by ERC Grant 617060. U87MG-R was kindly provided by Dr. W. Leenders (Radboud University, Nijmegen).

Appendix A. Supplementary data

Supplementary data associated with this article can be found, in the online version, at http://dx.doi.org/10.1016/j.radonc.2015.06.020.

References

[1] Stupp R, Mason WP, van den Bent MJ, Weller M, Fisher B, Taphoorn MJ, et al. Radiotherapy plus concomitant and adjuvant temozolomide for glioblastoma. N Engl J Med 2005;352:987–96.
[2] Oliva CR, Nozell SE, Diers A, McClugage 3rd SG, Sarkaria JN, Markert JM, et al. Acquisition of temozolomide chemoresistance in gliomas leads to remodeling of mitochondrial electron transport chain. J Biol Chem 2010;285:39759–67.
[3] Howes AL, Chiang GG, Lang ES, Ho CB, Powis G, Vuori K, et al. The phosphatidylinositol 3-kinase inhibitor, PX-866, is a potent inhibitor of cancer cell motility and growth in three-dimensional cultures. Mol Cancer Ther 2007;6:2505–14.
[4] Carlsson J, Acker H. Relations between Ph, oxygen partial-pressure and growth in cultured-cell spheroids. Int J Cancer 1988;42:715–20.
[5] Eke I, Cordes N. Radiobiology goes 3D: how ECM and cell morphology impact on cell survival after irradiation. Radiother Oncol 2011;99:271–8.
[6] Verhaegen F, van Hoof S, Granton PV, Trani D. A review of treatment planning for precision image-guided photon beam pre-clinical animal radiation studies. Z Med Phys 2014;24:323–34.
[7] Yahyanejad S, Granton PV, Lieuwes NG, Gilmour L, Dubois L, Theys J, et al. Complementary use of bioluminescence imaging and contrast-enhanced micro-computed tomography in an orthotopic brain tumor model. Mol Imaging 2014;13:1–8.
[8] Hiddingh L, Tannous BA, Teng J, Tops B, Jeuken J, Hulleman E, et al. EFEMP1 induces gamma-secretase/Notch-mediated temozolomide resistance in glioblastoma. Oncotarget 2014;5:363–74.
[9] van Hoof SJ, Granton PV, Verhaegen F. Development and validation of a treatment planning system for small animal radiotherapy: SmART-Plan. Radiother Oncol 2013;109:361–6.
[10] Niyazi M, Geisler J, Siefert A, Schwarz SB, Ganswindt U, Garny S, et al. FET-PET for malignant glioma treatment planning. Radiother Oncol 2011;99:44–8.
[11] Chang J, Thakur SB, Huang W, Narayana A. Magnetic resonance spectroscopy imaging (MRSI) and brain functional magnetic resonance imaging (fMRI) for radiotherapy treatment planning of glioma. Technol Cancer Res Treat 2008;7:349–62.
[12] Zietarska M, Maugard CM, Filali-Mouhim A, Alam-Fahmy M, Tonin PN, Provencher DM, et al. Molecular description of a 3D in vitro model for the study of epithelial ovarian cancer (EOC). Mol Carcinog 2007;46:872–85.
[13] Barbone D, Yang TM, Morgan JR, Gaudino G, Broaddus VC. Mammalian target of rapamycin contributes to the acquired apoptotic resistance of human mesothelioma multicellular spheroids. J Biol Chem 2008;283:13021–30.
[14] Brandes AA, Basso U, Reni M, Vastola F, Tosoni A, Cavallo G, et al. First-line chemotherapy with cisplatin plus fractionated temozolomide in recurrent glioblastoma multiforme: a phase II study of the Gruppo Italiano Cooperativo di Neuro-Oncologia. J Clin Oncol 2004;22:1598–604.